

MSEC2009-84113

SINGLE POINT DIAMOND TURNING EFFECTS ON SURFACE QUALITY AND SUBSURFACE DAMAGE IN CERAMICS

Deepak Ravindra

Mechanical Engineering
Western Michigan University
Kalamazoo, MI-49008, USA.
deepak.ravindra@wmich.edu

John A. Patten

Manufacturing Engineering
Western Michigan University
Kalamazoo, MI-49008, USA.
john.patten@wmich.edu

Jun Qu

Material Science & Technology Division
Oak Ridge National Laboratory
Oak Ridge, TN-37831
qujn@ornl.gov

ABSTRACT

Advanced ceramics, such as Silicon Carbide (SiC) and Quartz, are increasingly being used for industrial applications. These ceramics are hard, strong, inert, and light weight. This combination of properties makes them ideal candidates for tribological, semiconductor, MEMS and optoelectronic applications respectively. Manufacturing these materials without causing surface and subsurface damage is extremely challenging due to their high hardness, brittle characteristics and poor machinability. Often times, severe fracture can result when trying to achieve high material removal rates during machining of SiC or quartz due to their low fracture toughness. This research demonstrates that ductile regime Single Point Diamond Turning (SPDT) is possible on these materials to improve its surface quality without imparting subsurface damage. Machining parameters, such as depth of cut and feed, used to carry out ductile regime machining will be discussed. Subsurface damage analysis was carried out on the machined samples using non-destructive methods such as Optical Microscopy, Raman Spectroscopy and Scanning Acoustic Microscopy to show evidence that the chosen material removal method leaves a damage-free surface and subsurface. Optical microscopy was used to image the improvements in surface finish whereas Raman spectroscopy and scanning acoustic microscopy was used to observe the formation of amorphous layer and subsurface imaging in the machined regions. All three techniques complement the initial hypothesis of being able to remove a nominally brittle material in the ductile regime.

INTRODUCTION

Silicon carbide is used in specialized industries due to its excellent mechanical properties such as extreme hardness, high wear resistance, high thermal conductivity, high electric field breakdown strength and high maximum current density.¹

The fully dense cubic (beta) polycrystalline silicon carbide (manufactured by POCO Graphite) CVD coating ($\approx 250\mu\text{m}$ thick) is a potential candidate to be used as mirrors for surveillance, high energy lasers (such as airborne laser), laser radar systems, synchrotron x-ray, VUV telescopes, large astronomical telescopes and weather satellites.² The primary reasons CVD coated silicon carbide is preferred for these applications is that the material possesses high purity ($>99.9995\%$), homogeneity, density (99.9% dense), chemical and oxidation resistance, cleanability, polishability and thermal and dimensional stability. Machining silicon carbide is extremely challenging due to its extreme hardness ($\approx 27\text{ GPa}$) and brittle characteristics. Besides the low fracture toughness of the material, severe tool wear of the single crystal diamond tool also has to be considered.

Quartz, also known as silicon dioxide (SiO_2), is the most abundant nonmetallic mineral on earth. There are several forms of quartz such as quartz crystals, natural fused silica (amorphous form of SiO_2) and synthetic fused silica (polycrystalline). For this research experiment, a synthesized fused silica (Spectrosil 2000.³) was used. Spectrosil 2000 is an ultra pure synthetic fused silica manufactured by Saint-Gobain Quartz PLC. This quartz material has a wide optical range from 180nm in the deep ultra violet transmission through to 2000nm in the infrared (IR). This material possesses a chemical purity of 99.999% and is manufactured using an environmentally friendly process, which results in a material that is both chlorine-free and bubble-free. A 6" diameter round disk was obtained in order to carry out the SPDT experiments.

The mechanics of material removal in SiC and glass (Quartz) can be classified in two categories: brittle fracture and plastic deformation. Good optical quality surfaces can be achieved by removing the material in a ductile manner. The work of past researchers suggests that glasses do not

necessarily behave as brittle material (even at room temperature) especially in the nanometric scale.^{4,5,6} The strength, hardness and fracture toughness of the work piece material are the governing factors that control the extent of brittle fracture.⁷ Some studies include detailed observations of a small amount of plastic deformation in brittle materials during a precision machining operation.⁸

Previous researchers have successfully been able to precisely grind CVD-SiC (using high precision grinding) but this process is very expensive and the fine abrasive wheels often result in an unstable machine/process.⁹ Single point diamond turning (SPDT) was chosen as the material removal method as SPDT offers better accuracy, quicker fabrication time and lower cost when compared to grinding and polishing.^{10,11} Although SiC and Quartz are naturally brittle, micromachining these materials are possible if sufficient compressive stress is generated to cause a ductile mode behavior, in which the material is removed by plastic deformation, instead of brittle fracture. This micro-scale phenomenon is also related to the High Pressure Phase Transformation (HPPT) or direct amorphization of the material.¹² The plastic deformation or plastic flow of the material, at the atomic to micro scale, occurs in the form of severely sheared machining chips caused by highly localized contact pressure and shear.

EXPERIMENTAL METHOD

The equipment used to carry out all of the machining experiments was the Micro-Tribometer (UMT) from the Center for Tribology Research Inc. (CETR). This equipment was developed to perform comprehensive micro-mechanical tests of coatings and materials at the micro scale. *Figure 1* shows the equipment setup for the 6" CVD coated SiC disk. A similar setup was used to carry out SPDT experiments on the 6" Quartz disk. A single crystal diamond tool with a 3mm nose radius, -45 degree rake angle and 5 degree clearance angle was used for the cutting tests. The MASTERPOLISH 2 Final Polishing Suspension (contains alumina and colloidal silica with a pH ~9) from Buehler, Inc. was used as the cutting fluid for all experiments involving diamond turning SiC.¹³ Likewise, all machining for the Quartz piece was done under wet conditions using the MASTERMET 2 Colloidal Silica Suspension from Buehler Inc. This cutting fluid (obtained from Buehler, Inc.) contains fine, noncrystallizing (0.02 μ m) SiO₂ particles in an aqueous base that is suitable for machining quartz/glass.¹³



Figure 1: Machining Setup for the 6" CVD coated SiC disk

SPDT of the 6" CVD Coated SiC

The preliminary single point diamond turning experiments were successful in reducing the surface roughness of a CVD coated silicon carbide disk.¹⁴ The Ra was brought down by over one order of magnitude (*from 1158nm to 83nm*). Since the goal of this research was to develop machining parameters appropriate for ductile mode machining of CVD SiC, there were several additional steps (machining passes) that had to be carried out in order to confirm or verify the processing parameters. For the actual manufacturing process, many steps (passes) were eliminated to make the actual production process more cost and time efficient¹⁵.

Pass	Programmed Depth of Cut	Actual Depth of Cut	Feed (μ m/rev)
1	2 μ m	1.3 μ m	30
2	2 μ m	1.2 μ m	30
3	2 μ m	845nm	5
4	500nm	255nm	1
5	500nm	210nm	1
6	500nm	160nm	1

Table 1: Recommended machining parameters for improving surface quality of a CVD coated SiC disk by SPDT. The actual measured depth of cut is within a 5% error margin.

A total of 6 passes have been suggested for the final manufacturing process to improve the surface roughness of silicon carbide. When an additional machining pass is found not to change/improve the surface roughness significantly, that pass is removed in the final recommendation as shown in *Table 1*. The actual depth of cut is always expected to be less than the programmed depth of cut (in most cases for SiC and Quartz, the actual depth of cut is about half of the programmed depth of cut) due to the elastic properties of the material and tool system. In this study, all analysis was based upon the actual measured depth of cut.

SPDT of Quartz (Spectrosil 2000)

After the preparatory/preliminary tests were carried out and analyzed, the final machining on the Spectrosil 2000 was conducted (preparatory results showed good signs of ductile mode machining). A total of two passes were carried out in order to achieve the target surface roughness (Ra < 50nm). The first pass was done at a 1 μ m programmed depth of cut with a 1 μ m/rev feed and the second pass was done at a 500nm programmed depth of cut with a 1 μ m/rev feed. The 1 μ m depth of cut was carried out as it showed ductile mode material removal behavior in the preparatory tests. A low feed (1 μ m/rev) was chosen to minimize brittle fracture and to improve the surface roughness.

The surface roughness was measured after each pass in order to finalize the machining conditions for the following pass (in this case the surface was analyzed after Pass 1 to decide the machining conditions for Pass 2). The diamond cutting tool was imaged and tool wear was measured and recorded. Cutting force (Fx) data was extracted in order to correlate it with the measured tool wear and achieved surface roughness. All of the final machining was done under wet

conditions using the MASTERMET 2 Colloidal Silica Suspension from Buehler Inc.

RESULTS

SPDT of the 6" CVD Coated SiC

All six machining passes carried out for the final machining experiment were successful. This section discusses the results for the final machining of the 6" CVD-SiC. *Figure 2* shows the surface roughness data for all passes.

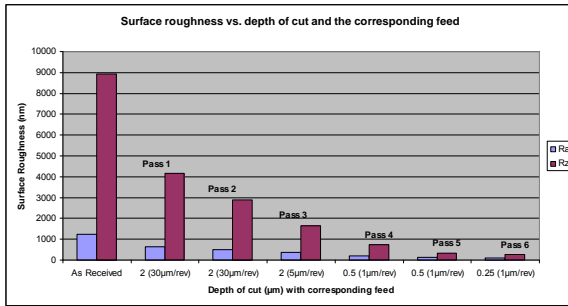


Figure 2: Surface roughness with their corresponding depth of cut and feed in parenthesis.

The results suggest that the surface roughness improved after every machining pass. The trend was consistent with the results obtained in the preliminary machining experiment where the Ra value decreased as the peak-to-valley (Rz) value decreased¹⁴. The surface roughness (Ra) was reduced from 1.23µm to 88nm in six passes. *Figure 3* shows the cutting force with the corresponding feed and depth of cut for all six passes.

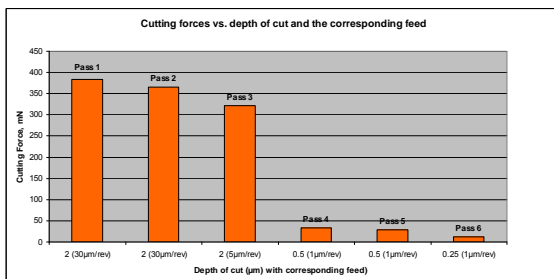


Figure 3: Cutting forces with their corresponding depth of cut and feed in parenthesis.

The cutting force consistently decreased after each pass. The main drop in cutting forces is observed in pass 4 due to the lower depth of cut. Cutting forces are a function of surface roughness (higher cutting forces due to rougher surfaces), depth of cut and feed. However, as seen in *Figure 3*, the most dominant parameter that influences the cutting force is the depth of cut (deeper cuts result in higher cutting forces).

The final study done for the machining tests was on the tool wear. *Table 2* shows the tool wear data for the respective machining conditions.

Pass	Fx (mN)	Depth of Cut (µm)	Feed (30µm/rev)	Length across the cutting radius (µm)	Rake Wear µm	Flank Wear µm
1	383.	2µm	30	370	6	36
2	365	2µm	30	360	4	29
3	322	2µm	5	343	3	27
4	33	500nm	1	220	2	14
5	28	500nm	1	218	2	11
6	11	250nm	1	155	2	9

Table 2: Tool wear data for the machining passes carried out. All measurements carried out are within a 5% error margin.

A new tool was used for every pass and there were no tool failures reported for any of the machining passes. In general, the tool wear data shows that the wear length across the cutting edge radius is directly proportional to the depth of cut (the deeper the depths of cut, the longer the measured wear across the cutting radius). The rake and flank wear are both a function of surface roughness, depth of cut and feed. In all six passes, the measured flank wear was more than the measured rake wear due to the larger contact area between the flank face of the tool and the workpiece.

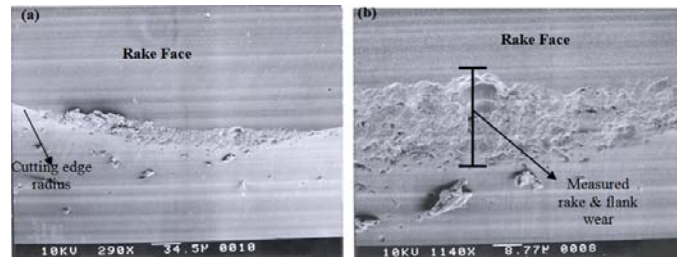


Figure 4 (a) & (b): SEM images of the cutting edge of the diamond tool after machining.

Figure 4(a) was taken at 290x and *Figure 4(b)* was taken at 1140x. This tool was used in for Pass #1 (also known as the roughing pass) where the programmed depth of cut was 2µm with a 30µm/rev feed. The large measured wear on the tool is due to the initial rough surface of the disk.

SPDT of Quartz (Spectrosil 2000)

A total of two passes were required in order to achieve the desired surface roughness (Ra < 50nm). The results in *Figure 5* suggest that the surface roughness consistently improved after each pass.

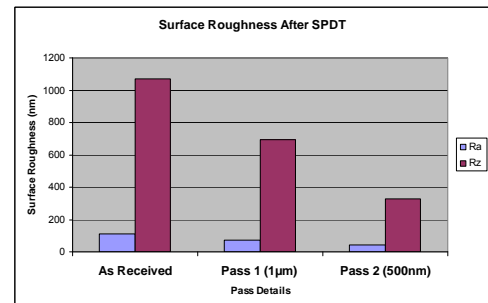


Figure 5: Chart comparing the as-received surface roughness with passes 1 and 2.

The data in *Figure 5* indicates that the surface roughness (in terms of Ra and Rz) had improved after both machining passes. After pass 2, the final surface roughness was measured to be 41nm (Ra) which is lower than the targeted Ra value. The depth of cut was decreased (from 1 μ m to 500nm) for the second pass as the peak-to-valley value was much lower than the as received surface (in general the program depth of cut is approximately equal to the Rz value). Also, a deeper cut could worsen the surface by causing more valleys (feed marks or grooves) on the workpiece surface.

Programmed Depth of Cut	Actual Depth of Cut	Feed	Thrust Force (Fz)	Cutting Force (Fx)	Force Ratio
1 μ m	651nm	1 μ m/rev	115mN	13.17mN	0.11
500nm	363nm	1 μ m/rev	50.25mN	5.65mN	0.11

Table 3: Table of the parameters used to machine the Spectrosil 2000. The measured depth and cutting forces are within a 5% error margin. The thrust force measurement is within a 2% error margin.

The thrust (Fz) force was an input value used to obtain the required depth of cut and the cutting force (Fx) was an output value measured during the turning operation. $Fz(\sigma)$ is the std dev of the thrust force. Force ratio is (Fx/Fz). The data in *Table 3* above indicates that the forces (both thrust and cutting) were stable throughout the entire machining operation resulting in a standard deviation of less than 7% ($Fz(\sigma)$). As mentioned in the previous section, it is important to obtain stable forces in order to produce a uniform cut. The force ratio (Fx/Fz) for both cuts were consistent (0.11), indicating uniformity in both cuts/passes. The second pass had lower cutting forces due to a lower depth of cut and a smoother surface to start off with (in general smaller forces are preferred). The actual depth of cut for both passes were less than the programmed depth of cut due to the elastic properties of the material (this elasticity effect was expected and is consistent with the work done on the 6" CVD-SiC)¹⁴. The surface roughness data and surface images (*Figures 6&7*) suggest that material was removed in the ductile mode even at the 651nm depth of cut (actual measured depth of cut). This conclusion is reasonable as past researchers have indicated pure ductile material removal below a depth of cut of 1 μ m.¹⁶ These same authors, Q.L. Zhao et al., also stated in their research that for any cuts from 1 μ m to 3.5 μ m, the starting of brittle material removal is observed as micro-cracks form on the surface.

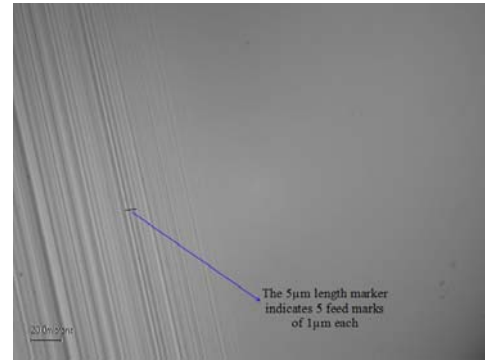


Figure 6: The optical microscope image shows the feed marks of the machined region (left) after pass 1.

The unmachined region (right) in *Figure 6* has no marks. This image was taken at a 400x magnification.

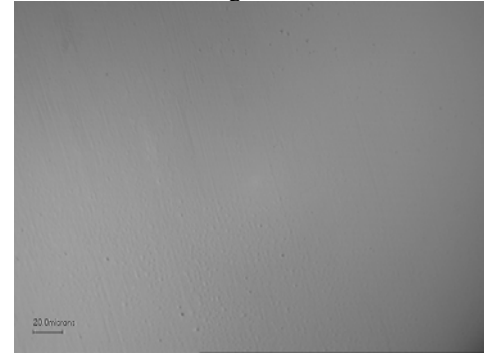


Figure 7(a): Image at 400x magnification showing very light feed marks on the machined region (left side of image) after pass 2.



Figure 7(b): Image at 1000x magnification showing very light feed marks on the machined region (left side of image) after pass 2.

The unmachined region in *Figures 7(a) and 7(b)* (right side) has no feed marks. These images were taken at a 400x and 1000x magnification respectively. Comparing *Figures 6* and *7(a) and (b)*, it is obvious that the resultant surface obtained after pass 2 is better than the machined surface after pass 1. This complements the surface roughness data obtained after each pass, as shown in *Table 3*. The feed marks caused in pass 1 have been removed after pass 2, resulting in a much smoother surface.

SUBSURFACE DAMAGE ANALYSIS

It is known that during hardness indentation, ceramics are subjected to highly localized stresses that not only could cause crack formation and plastic deformation but also a change in crystal structure and formation of an amorphous phase.¹⁷ This similar concept of contact induced pressure also applies while cutting as ceramics undergo an extremely high pressure phase transformation during machining¹⁸. Due to the high pressure phase phenomenon, it is possible that subsurface damage occurs in these brittle materials without any indication of surface damage. Two different non destructive techniques were used to investigate the subsurface damage of the machined SiC; laser micro-Raman spectroscopy and scanning acoustic microscopy (SACM).

Laser micro-Raman Spectroscopy

Laser Raman spectroscopy is a well known non destructive characterization technique often used for semiconductors. Most of the past research and available literature show that Raman spectroscopy has been used to study machined silicon surfaces, spherical, conical, or pyramid diamond tips or indenters^{19,20}. However, in this study, Raman spectroscopy proved to be successful in observing phase transformation of a diamond turned SiC workpiece. A 633nm wavelength He-Ne laser was used to study the subsurface of the machined. The main purpose of the Raman spectroscopy in this study is an attempt to detect the amorphous layer beneath the machined surface.

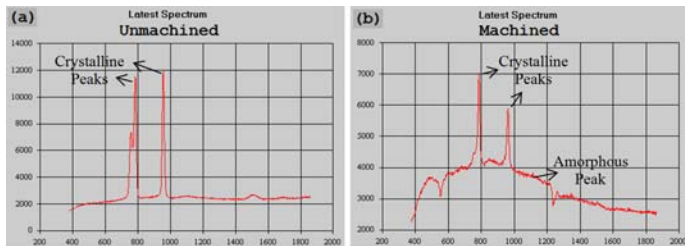


Figure 8: Micro-Raman laser spectrum of the unmachined SiC (a) and the machined SiC (b) surfaces.

In *Figure 8(a)*, the spectrum shows the crystalline peaks of the unmachined SiC sample. Comparing these peaks with *Figure 8(b)*, it is seen that a combination of the crystalline peaks (sharp peaks) and amorphous peaks (broadband peaks) are formed in the machined surface. The amorphous layer is a good indication of a ductile material removal process²¹. In general, the thickness of the amorphous layer increases as the depth of cut is increased.²²

Scanning Acoustic Microscopy (SACM)

SACM is widely used in non-destructive evaluation (NDE) of materials utilizing high-frequency acoustic waves (60MHz to 2.0GHz) to reveal surface topography, subsurface features and elastic properties.²³ The Kramer Scientific Instruments (KSI) SAM2000 scanning acoustic microscope at the Oak Ridge National Laboratory (ORNL) was used for this study to investigate subsurface cracks and fracture after SPDT, if any. The concept of SACM is schematically illustrated in *Figure 9*. Acoustic waves are produced by a transducer, pass

through the coupling liquid (usually distilled water), and reflect from the focal plane (located at a distance 'z' below the specimen's surface). The reflected acoustic echoes from individual regions are detected during scanning and are used to assemble images.^{23,24}

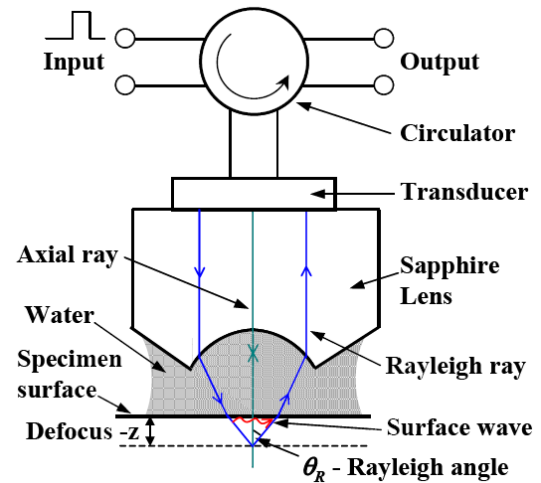


Figure 9: Schematic diagram of scanning acoustic microscopy.²³

The machined depth of 500nm is the investigated area in this section. The acoustic microscopy images show no sign or indication of subsurface cracks or damage as deep as 1.5 μm , except normal surface features and feed marks. The pits and voids seen in *Figure 10* existed in the as-received material and were not caused by the SPDT operation. Machining-induced damage would tend to fade off as the scan gets deeper, if there were any.

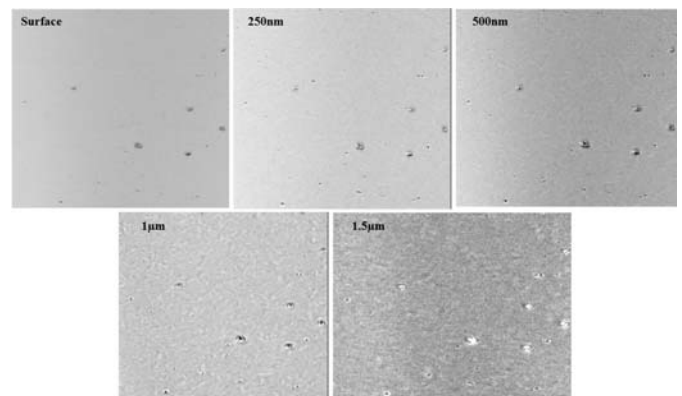


Figure 10: A sequence of images (each imaging an area of 150x150 μm) of the machined SiC sample (first image shows the surface and the numbers on the top left of each image represents the scanned depth beneath the machined surface).

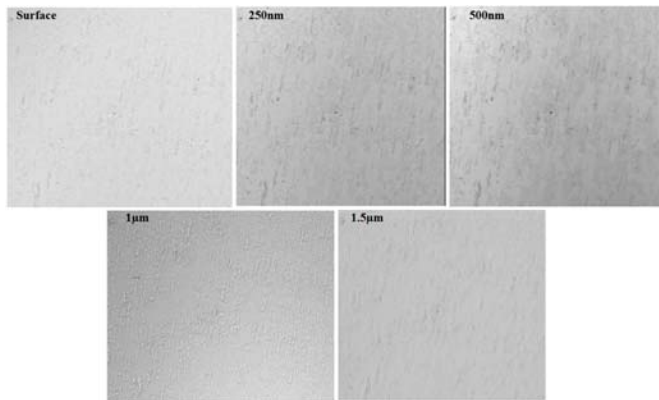


Figure 11: A sequence of images (each imaging an area of $150 \times 150 \mu\text{m}$) of the machined Quartz sample (first image shows the surface and the numbers on the top left of each image represents the scanned depth beneath the machined surface).

CONCLUSION

The single point diamond turning experiments were successful in reducing the surface roughness of a CVD coated silicon carbide and Quartz disks. The R_a was brought down by two orders of magnitude (*from $1.23 \mu\text{m}$ to 88nm*) for SiC and from 110nm to 41nm for Quartz. The most important consideration when machining in the ductile regime is not to exceed the critical depth or the ductile-to-brittle transition (DBT) depth of the material, in order to avoid brittle fracture, which leads to higher surface roughness. It is possible to machine nominally brittle materials by plastic deformation at small scales i.e. below the critical depth or the below the DBT.

The best surface finish was obtained with the lowest feed rate attempted ($1 \mu\text{m}/\text{rev}$) but initially a higher feed rate was used ($30 \mu\text{m}/\text{rev}$ for SiC) to maximize the material removal rate and minimize tool wear. The trade off at lower feed rates is that the measured tool wear is much more than at the higher feeds as shown in the results, but the resultant surface finish is improved. The tool wear can be reduced by using suitable cutting fluids to reduce frictional effects and also by reducing the feed rates once the surface becomes smooth.

Micro Raman spectroscopy and SAcM were both proven to provide useful information that supported the fact that even hard brittle materials can be machined in the ductile regime. Micro Raman was used to identify the phase transformation (detect an amorphous phase in SiC) where as SAcM was used to investigate subsurface damage. Both non-destructive techniques showed complimenting results where no signs of brittle material removal was detected. Since the machined Quartz sample is optically transparent, optical microscopy (by simple adjusting the focal distance of the lens) was also used to investigate subsurface damage just beneath the machined surface. SPDT was successful in improving the surface of SiC and Quartz without causing surface and subsurface damage.

REFERENCES

- ¹ Deepak Ravindra, John Patten and Makoto Tano, 2007, "Ductile to Brittle Transition in a Single Crystal 4H SiC by Performing Nanometric Machining", ISAAT 2007 Precision Grinding and Abrasive Technology at SME International Grinding conference, Advances in Abrasive Technology, X, pp 459-465.
- ² Biswarup Bhattacharya, 2005, "Ductile Regime Nano-Machining of Polycrystalline Silicon Carbide", Masters Theses, Western Michigan University.
- ³ <http://www.quartz.saintgobain.com/Media/Documents/S0000000000001011/Spectrosil%20Optical%20Fused%20Silica.pdf>
- ⁴ Y. Ishida, G. Ogawa, 1962, Japanese Journal of Mechanical Engineering Laboratory, v.8, (1), pp.15-30.
- ⁵ D.M. Marsh, 1964, "Plastic Flow and Fracture of Glass", Proc. R. A, v.282, pp.33-43.
- ⁶ F.M. Ernsberger, 1968, "Glasses Under Point Loading", Journal of the American Ceramic Society, v.51, pp.545-547.
- ⁷ R. Komanduri, 1996, "On Material Removal Mechanisms in Finishing of Advanced Ceramics and Glasses", Annals of the CIRP (College International pour la Recherche en Productique), v.45, p.509.
- ⁸ M.A. Moore, F.S. King, 1980, "Abrasive Wear of Brittle Solids", Wear, v.60, pp.123-130.
- ⁹ Chunhe Zhang, Teruko Kato, Wei Li and Hitoshi Ohmori, 2000, "A Comparative Study: Surface Characteristics of CVD-SiC Ground with Cast Iron Bond Diamond Wheel", International Journal of Machine Tools and Manufacture, v.40, pp. 527-537.
- ¹⁰ F.Z. Fang, X.D. Liu and L.C. Lee, 2003, "Micro-machining of Optical Glasses- A Review of Diamond- Cutting Glasses", Indian Academy of Sciences, v.28, Part 5.
- ¹¹ John Patten and Bis Bhatt, 2006, "Single Point Diamond Turning of CVD Coated Silicon Carbide", ASME MSEC.
- ¹² John A. Patten, W. Gao and K. Yasuto, 2005, "Ductile Regime Nanomachining of Single-Crystal Silicon Carbide", ASME, v.127, pp.522- 532.
- ¹³ http://www.buehler.com/productinfo/consumables/pdfs/FINAL_POLISHING.pdf
- ¹⁴ Deepak Ravindra and John Patten, "Improving the Surface Roughness of a CVD Coated Silicon Carbide Disk by Performing Ductile Regime Single Point Diamond Turning", Proceedings of the 2008 International Manufacturing Science and Engineering Conference, Michigan.
- ¹⁵ F.Z. Fang, X.D. Liu, L.C. Lee, 2003, "Micro-machining of Optical Glasses- A Review of Diamond- Cutting Glasses", Indian Academy of Sciences, v.28, Part 5.
- ¹⁶ Q.L. Zhao, D. Stephenson, J. Corbett, J. Hedge, J.H. Wang and Y.C. Liang, 2004, "Single Grit Diamond Grinding of Spectrosil 2000 Glass on Tetraform 'C'", Advances in Abrasive Technology VI, v.257-258, pp.107-112.
- ¹⁷ Andreas Kailer, Klaus G. Nickel and Yury G. Gogotsi, 1999, "Raman Microspectroscopy of Nanocrystalline and Amorphous Phase in Hardness Indentations", Journal of Raman Spectroscopy, v.30, pp.939-946.

¹⁸ M. Yoshida, M. Ueno, K. Takemura and O. Shimomura, 1993, "Pressure Induced Phase Transition in SiC", The American Physical Society, v.48, n.14, pp. 587-590.

¹⁹ B.V. Tanikella, A.H. Somasekhar, A.T. Sowers, R.J. Nemanich and R.O. Scattergood, 1996, Appl. Phys. Lett. , V.69, pp.2870.

²⁰ Yuri Gogotsi, G. Zhou, S. Ku and S. Cetinkunt, 2001, Semiconductor Science Technology, v.16, pp. 345.

²¹ Y.G. Gogotsi, A.Kailer and K.G.Nickel, 1997, "Phase Transformations in Materials Studied by Micro-Raman Spectroscopy of Indentations", Materials Reserve Innovations, v1, pp 3-9.

²² Jiwang Yan, Tooru Asami and Tsunemoto Kuriyagawa, 2008, "Nondestructive Measurement of Machining-Induced Amorphous Layers in Single-Crystal Silicon by Laser Micro-Raman Spectroscopy", Journal of Precision Engineering, v.32,pp.186-195.

²³ Jun Qu, Peter J. Blau, Albert Shih, Samuel McSpadden, George Pharr and Jae-il Jang, 2004, "Scanning Acoustic Microscopy for Non-Destructive Evaluation of Subsurface Characteristics", Proceedings of the 6th International Conference on Frontiers of Design and Manufacturing (S.M. Wu Symposium on Manufacturing Sciences), Xi'an, China, Paper #435.

²⁴ Jun Qu and Peter J. Blau, "Scanning Acoustic Microscopy for Characterization of Coatings and Near-Surface Features of Ceramics", 2006, Proceedings of the 30th International Conference & Exposition on Advanced Ceramics and Composites, Cocoa Beach, Florida, pp. 22-27.